Weierstraß-Institut

für Angewandte Analysis und Stochastik

Leibniz-Institut im Forschungsverbund Berlin e. V.

Quasi-phase-matching for third harmonic generation in noble gases employing ultrasound

Usman K. Sapaev[1], Ihar Babushkin[2], Joachim Herrmann[1]

submitted: 14 Dec 2012

[1] Max Born Institute
   for Nonlinear Optics
   and Short Time
   Spectroscopy
   Max-Born-Str. 2A
   12489 Berlin
   Germany

[2] Weierstrass Institute
   Mohrenstr. 39
   10117 Berlin
   Germany
   E-Mail: ihar.babushkin@wias-berlin.de

Abstract

We study a novel method of quasi-phase-matching for third harmonic generation in a gas cell using the periodic modulation of the gas pressure and thus of the third order nonlinear coefficient in the axial direction created by an ultrasound wave. Using a comprehensive numerical model we describe the quasi-phase matched third harmonic generation of UV (at 266 nm) and VUV pulses (at 133 nm) by using pump pulses at 800 nm and 400 nm, respectively, with pulse energy in the range from 3 mJ to 1 J. In addition, using chirped pump pulses, the generation of sub-20-fs VUV pulses without the necessity for an external chirp compensation is predicted.

1 Introduction

Third harmonic generation (THG) in gases is a method with one of the simplest setup allowing to generate picosecond and femtosecond pulses in the UV and VUV spectral ranges. Compared with alternative schemes employing solid-state crystals several disadvantages can be avoided by using gases such as low damage threshold, strong dispersion, bandwidth limitations and restrictions of the spectra to the range above 200 nm. For intensities below the ionization threshold THG cannot take place for pump beams focused into a gas cell because the emitted third harmonic (TH) before the focus cancels the one emitted after the focus [1, 2] due to destructive interference. This problem can be avoided by placing the gas cell before or after the focus [1, 2], by using a differentially pumped gas cell, a narrow gas jet [3], or hollow waveguides [4, 5]. THG during ultrafast ionization with higher efficiencies has been generated by focusing the pump beam inside a chamber with a noble gas with intensities far in excess of that necessary for ionization [6–8]. TH has also been generated during filamentation of femtosecond pulses in air and argon [9–14]. Several papers reported that the efficiency of THG in a filament can be increased by using a second intercepting IR pulse [11–14], which can be explained by the quenching of interference effects [14].

One of the main difficulties, limiting the efficiency in frequency conversion in the above described methods is the problem to realize phase-matching. In UV and VUV pulse generation in hollow waveguides by four-wave mixing phase-matching can be realized using the anomalous dispersion of the fiber [15–17]. However, the small diameter of the capillary limits the pulse energy and leads to more complexity in practical realization. In the case of frequency conversion in solid nonlinear crystals an alternative approach, quasi-phase matching (QPM), is used. It exploits a periodic modulation of the nonlinear susceptibility to correct the linear phase mismatch [18, 19]. For the application in high-order harmonic generation in gas-filled hollow waveguides QPM was demonstrated by using modulated hollow-core waveguides [20] or using counter-propagating light [21, 22].

1

In this paper, we investigate a novel technic for quasi-phase matching by ultrasound in THG. As presented in Fig. 1 in this scheme a cell filled with a noble gas is excited by a pump pulse and an ultrasound wave which modulates the gas pressure and thus the third order nonlinearity of the gas. For an ultrasound wave-number approximately equal to the module of the linear phase mismatch between the fundamental and the generated TH QPM can be realized, greatly increasing the conversion efficiency. Since the beam diameter is not limited as in hollow waveguides, this method allows the use of very high pump energies with larger diameters for frequency transformation into the VUV. Here we study THG in an argon-filled cell with the pump wavelength at 800 nm for UV and at 400 nm for VUV pulses generation with moderate and high pump energies up to the joule level. Using a comprehensive nonlinear model including the influence of dispersion, diffraction, third-order nonlinearity, ionization as well as the sound loss, we show that the conversion efficiency can be increased as a result of QPM. In particular, we show the possibility that by using pre-chirped femtosecond pump pulses at 400 nm sub-20 fs VUV pulses can be generated. Intriguingly, due to the normal dispersion of the gas the generated VUV pulse at the output is nearly unchirped and thus does not need any additional chirp compensation stage.

Figure 1: QPM for THG using an ultrasound wave. (a) - The basic scheme: the pump with frequency ω is sent into a tube where an ultrasound wave is exited to achieve the QPM. At the output, third harmonic 3ω is observed. (b) - Dependence of the ultrasound frequency Ω_s on the pump wavelength λ for THG QPM in argon at 1 atm. (c) - The absorption rate of the ultrasound wave in argon at the normal conditions in dependence on its frequency Ω_s.

2   Quasi-phase matching using ultrasound

QPM is a technic to correct the phase mismatch between interacting waves without matching the phase velocities. QPM in periodically poled nonlinear crystals is realized by a nonlinear structure in which the sign of the nonlinear susceptibility is periodically reversed throughout the medium [18, 19]. However, QPM can also be realized by a periodic modification of the nonlinear coefficient without sign change. A method for QPM in isotropic gases was described in [23], in which an ultrasound transducer in a gas cell excites ultrasound waves which periodically change the pressure or, in other words, the particles number density and therefore the third-order nonlinear susceptibility. The ultrasound wavevector K_s required to achieve QPM of interacting waves in the cell is approximately equal to the phase-mismatch $|\Delta\mathbf{k}|$ due to dispersion of the corresponding waves. In this paper we study in detail THG as a simplest prototypical interaction (see Fig. 1). In this case the phase mismatch is given by $\Delta\mathbf{k} = \mathbf{k}_{3\omega} - 3\mathbf{k}_\omega$, where $\mathbf{k}_\omega$ is the pump wavevector with the frequency ω and $\mathbf{k}_{3\omega}$ is the TH wavevector with the frequency 3ω. The dependence of the ultrasound frequency $\Omega_s = 2\pi/K_s$ on the pump wavelength $\lambda = 2\pi/\omega$ is shown in Fig. 1(b). As seen for argon QPM for THG with a pump pulse at 800 nm requires an ultrasound frequency of $\Omega_s \approx 22$ kHz and for a pump pulse at 400 nm we find $\Omega_s \approx 300$ kHz. For high intensities the Kerr effect introduces an additional phase shift.

Ultrasound waves can be efficiently generated by the application of piezoelectric generators. In liquids, high power ultrasound waves up to tens of MHz are heavily used in many applications

2

in technology, medicine, biology and chemistry [24]. In contrast, in gases typical high-power ultrasound devices rarely exceed ~ 40 kHz limit. However, some ultrasonic applications such as nondestructive testing require airborn ultrasound from 100 kHz up to 1 MHz. In such applications, the pressure amplitudes p in a pulsed regime can achieve $\sim 10^{-2}$ atm inside the area of ~ 1 cm^2 [25]. Even using relatively common airborn high-power ultrasound source with frequency around 20 kHz, higher frequencies can be obtained as harmonics of the fundamental one. In particular, in [26], high power (200 W) cw ultrasound with high pressure level ≈ 160 dB (this corresponds to $p \sim 10^{-2}$ atm) was excited in air at atmospheric pressure for a transducer with resonant frequency $\Omega_s = 20$ kHz. Due to nonlinearities of generation and propagation, the ultrasound contained higher harmonics; in particular, the contribution of fourth-order harmonic ($\Omega_s = 80$ kHz) in this wave was estimated to be up to ≈ 130 dB ($p \approx 5 \times 10^{-4}$ atm).

The propagation of sound wave in a tube is relatively well studied [27, 28]. If the viscous effects from the walls can be neglected (the case of "wide tube"), the fundamental sonic mode in a waveguide is homogeneous across the direction transverse to the propagation one. Such mode have also a free-space dispersion and negligible waveguide-induced losses. In the case when viscosity effects becomes important (the case of "narrow tube"), the situation changes. Viscosity leads to the occurring of a boundary layer, with pressure variations decreasing to zero at the walls, and also to additional losses. The role of viscosity is determined by the so called shear wave number $s = \frac{D}{2}\sqrt{\frac{\Omega_s}{\nu}}$ [27, 28] where D is the tube diameter, ν is the kinematic viscosity. Viscosity effects become important for $s \leq 1$. For typical parameters considered in the present article (atmospheric pressure, $\Omega_s = 0.3$ MHz) and assuming reasonable tube diameter of $\approx$ 1 cm ([25]) we obtain $s \sim 3 \times 10^3$, that is the approximation of "wide tube" is very well applicable. For the above mentioned parameters, the losses induced by the tube itself are of order of 5×10^{-2} cm^{-1}, according the model introduced in [28].

Even in a free space the high frequency ultrasound has noticeable decay, which is in the case of noble gas can be described by the formula [29, 30]:

$$\beta_s = \frac{\Omega_s^2}{8\pi^2 \rho_0 c_s^3}\left(\frac{4}{3}\eta + (\gamma - 1)\frac{\kappa}{C_p}\right), \tag{1}$$

where ρ_0 is the gas atomic density, c_s is the sound speed, κ is the thermal conductivity, η is the shear viscosity, $\gamma = C_p/C_v$ is the rate of the heat capacity at constant pressure (C_p) and constant volume (C_v).

The dependence of the loss coefficient β_s on the ultrasound frequency Ω_s for argon is shown in Fig. 1(c). Although the losses given by the classical formula Eq. (1) are underestimated for liquids and multi-atomic gases, Eq. (1) works still reasonably good for noble gases [29–31].

According to the facts mentioned above, the gas pressure can be described in a simple way as a decaying plane wave along the propagation axis z: $P(x, y, z) = P_o + p(x, y)e^{-\beta_s z}\cos(K_S z)$. Here P_o is the background pressure and $p(x, y)$ is the ultrasound amplitude, which is constant inside the tube ($\sqrt{x^2 + y^2} \equiv r < D/2$) and zero otherwise (the "wide tube" approximation discussed above) that is, $p(x, y) \equiv p = $ const.

The propagation of the pump and TH in the gas-filled tube excited by the ultrasound wave can be described by a comprehensive model taking into account diffraction, dispersion, third-order nonlinearity, gas ionization effects and periodically changing pressure. Using the slowly varying

envelope approximation the amplitudes of the pump $A_\omega(x, y, z, t)$ and the TH $A_{3\omega}(x, y, z, t)$ as well as the free electron density $\rho(x, y, z, t)$ in time t and space are given by:

$$\frac{\partial A_\omega}{\partial z} + \widehat{M_\omega} A_\omega = i\gamma_\omega(z) \left\{ A_\omega \left(|A_\omega|^2 + 2 |A_{3\omega}|^2 - \Gamma_\omega \right) + A_\omega^{*2} A_{3\omega} e^{i\Delta kz} \right\}, \qquad (2)$$

$$\frac{\partial A_{3\omega}}{\partial z} + \widehat{M_{3\omega}} A_{3\omega} = i\gamma_{3\omega}(z) \left\{ A_{3\omega} \left(|A_{3\omega}|^2 + 2 |A_\omega|^2 - \Gamma_{3\omega} \right) + A_\omega^3 e^{-i\Delta kz}/3 \right\}, \qquad (3)$$

$$\frac{\partial \rho}{\partial t} = (\rho_o(z) - \rho) \left(\sigma_{K_\omega} |A_\omega|^{2K_\omega} + \sigma_{K_{3\omega}} |A_{3\omega}|^{2K_{3\omega}} \right) + \frac{\rho}{U_i} \left(\sigma_\omega(z) |A_\omega|^2 + \sigma_{3\omega}(z) |A_{3\omega}|^2 \right).$$
$$(4)$$

Here $\gamma_m(z) = \dfrac{3\pi m^2 \chi^{(3)}(z)}{2c^2 k_m^o}$ is the third order nonlinear coefficient ($m = \omega$ and 3ω for the fundamental and TH, correspondingly); $\chi^{(3)}(z)$ is the third-order nonlinear susceptibility, depending on the pressure P (and hence on z); Δk is the linear phase mismatch for the gas pressure P_0. $\widehat{M_\omega}$, $\widehat{M_{3\omega}}$ and Γ_ω, $\Gamma_{3\omega}$ are defined as:

$$\widehat{M_m} = -i \left(k_m(z) - k_m^o \right) + \nu_m(z) \frac{\partial}{\partial t} + \frac{ig_m(z)}{2} \frac{\partial^2}{\partial^2 t} - \frac{i}{2k_m(z)} \left[\frac{\partial^2}{\partial x^2} + \frac{\partial^2}{\partial y^2} \right], \qquad (5)$$

$$\Gamma_m = \frac{\sigma_m(z)}{2} (1 + i\omega_m^o \tau_c(z)) + \frac{\beta_{K_m}}{2} (\rho_o(z) - \rho) |A_m|^{2K_m - 2}, \qquad (6)$$

where $\nu_\omega = 0$ and $\nu_{3\omega}(z) = 1/V_\omega(z) - 1/V_{3\omega}(z)$; $V_m(z)$ and $g_m(z)$ are the group velocities and group velocity dispersions of the interacting pulses; $k_m(z)$ and k_m^o are the wave numbers for the (z-dependent) pressure P and for the background pressure P_0, respectively; $\sigma_m(z)$ is the cross section of inverse Bremsstrahlung; $\tau_c(z)$ is the free-carrier collision time; σ_{K_m} is the ionization cross section, where $K_m \equiv < U_i/\hbar\omega_m + 1 >$ here also U_i is the ionization potential of the gas; β_{K_m} is the multiphoton ionization coefficient, which is defined as $\beta_{K_m} = K_m \hbar\omega_m \sigma_{K_m}$; $\rho_o(z)$ is the density of neutral atoms [32, 33]. The coefficients $k_m(z)$, $\gamma_m(z)$, $V_m(z)$, $g_m(z)$, $\sigma_m(z)$, $\tau_c(z)$, are assumed here to be proportional to the pressure (and thus varying along the z-coordinate) [32–34].

Let us first consider the simplest approximation assuming an un-depleted pump pulse and neglecting diffraction, dispersion, ionization ($\Gamma_m = 0$) and loss, but taking into account the nonlinear self-phase modulation of the pump. Then, the on-axis QPM condition for the ultrasound wave vector K_s is:

$$K_S = \Delta k + 3\gamma_\omega |A_\omega^o|^2 - 2\gamma_{3\omega} |A_\omega^o|^2 \qquad (7)$$

where A_ω^o is the field amplitude of the pump at the input. If this condition is fulfilled and the weak non-phase matched contributions are neglected one obtains for the intensity of the third harmonic $I_{3\omega}$:

$$I_{3\omega}(z) \approx \frac{c\varepsilon_o(\gamma_{3\omega}pz)^2}{12} |A_\omega^o|^6. \qquad (8)$$

Remarkably, $I_{3\omega}$ does not depend on the background pressure P_0 but only on the ultrasound amplitude p.

For a more exact treatment we solved Eqs.$(2) - (4)$ numerically using the split-step method [35] with the fast Fourier transform in time and 2D transverse space dimensions to calculate the

linear part of the equations and the fifth-order Runge-Kutta method for the nonlinear one. In the solution of Eq. (4) the fourth-order Runge-Kutta method were used. The results of numerical simulations of Eqs. 2-4 for bandwidth-limited femtosecond and chirped picosecond pump pulses at 800 nm as well as at 400 nm are presented in the Chapter 3.

3   Results and their discussion

3.1   UV pulse generation by using 800 nm pump pulses

First, we studied the proposed method for a bandwidth-limited 800 nm Gaussian pump pulse with a duration (FWHM) $\tau_\omega = 700$ fs, a radius $r_\omega = 0.05$ cm and an energy 3 mJ (corresponding to the input intensity $I_o \approx 1$ TW/cm^2 and power $P_\omega \approx 3.97$ GW) with a sound amplitude of $p = 0.01$ atm. The required ultrasound frequency necessary to fulfill the QPM condition according Eq. (7) is $\Omega_s = 22.24$ kHz. For these parameters the self-focusing distance is $z_f \approx 11.01$ m, the critical power of self-focusing is $P_{crit} \approx 3.94$ GW and the walk-off length is $L_\nu = \tau_\omega/\nu \approx 345$ m. Therefore one can expect a relatively long propagation distance without beam collapsing, temporal walk-off or formation of a filament [36]. The results for these parameters are presented in Fig. 2. Figure 2 (a) shows the results of the analytical formula Eq. (8) (red dashed curve) and of the numerical simulations (red solid curve) for the efficiency of THG defined as $\eta_{3\omega}(z) = \iiint |A_{3\omega}(z,x,y,t)|^2 dxdydt / \iiint |A_\omega(z=0,x,y,t)|^2 dxdydt$. One can see from the Fig. 2(a) that QPM results in the efficient conversion to the TH at the optimum ultrasound frequency, which is 27 times larger than without ultrasound (green curve). The self-focusing effect is relatively weak as seen from the evolution of pump intensity (blue curve in Fig. 2(b)) and beam radius (red curve in Fig. 2(d)), while that spatial profile of the TH shows a good beam quality (Fig. 2(c)).
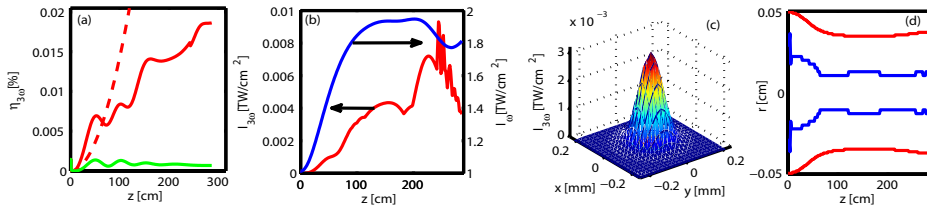

Figure 2: THG for a 0.7 ps pump pulse at 800 nm with 3 mJ energy. In (a) the conversion efficiency $\eta_{3\omega}$ calculated analytically by Eq. (8) (red-dashed) and numerically (red-solid) in dependence on the propagation distance z (the result in the absence of ultrasound is shown by the green curve); in (b) the evolution of the peak intensity of the pump (blue) and the TH (red); in (c) the spatial intensity profile of the TH at the output and in (d) the change of the radii of the pump (red) and the TH (blue) are presented.

Figure 3 shows the results for the case of a bandwidth-limited pump pulse at 800 nm with a high energy of 1 J, a duration of $\tau_\omega = 1$ ps (transform-limited), a radius of $r_\omega = 0.5$ cm and a sound amplitude of $p = 0.01$ atm. For these parameters one can calculate: $I_o \approx 2.4$ TW/cm^2, $z_f \approx 247$ cm, $L_\nu = \tau_\omega/\nu \approx 487$ cm. In this case the power of the pump pulse $P_\omega \approx 940$ GW
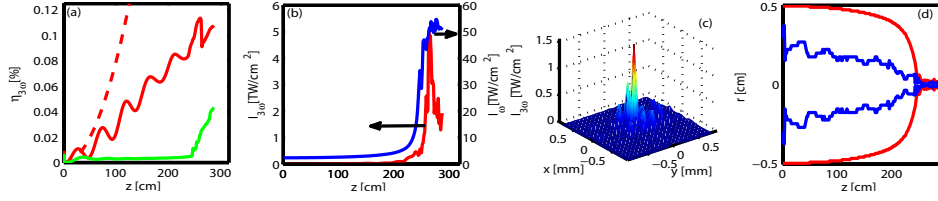
Figure 3: THG for a 1 ps pump pulse at 800 nm with 1 J energy. The description of (a)-(d) and the curves are analogous as Fig. 2.

is much larger than the critical power of self-focusing $P_{crit} \approx 3.94$ GW, therefore as seen in Fig. 3(d) after a propagation distance of about 2.5 m the pump beam radius significantly decreases and its intensity increases. The efficiency increases up to $\eta_{3\omega} \approx 0.12\%$, but due to the change of the pump intensity the QPM condition Eq. (7) is violated after this distance. Without ultrasound (green curve) the efficiency is at ~ 2.5 m 18 times smaller, but after self-focusing distance it increases significantly due to the increase of the pump intensity.

3.2   VUV pulse generation by using 400 nm pump pulses

Using THG with pump pulses at 400 nm allows frequency transformation into the VUV spectral range at 133 nm. Nowadays, generation of such pump pulses with high energy by second harmonic generation in nonlinear crystals from near-infrared ones is a standard method. Here we study THG with a bandwidth-limited pump pulse at 400 nm with 0.3 mJ energy, duration of $\tau_\omega = 1.4$ ps, beam radius of $r_\omega = 0.03$ cm, pump intensity $I_o \approx 1.4$ TW/cm^2 and sound amplitude of $p = 0.01$ atm. As one can see from the Fig. 4, the conversion efficiency increases up to the propagation length of about 50 cm. The saturation of THG is caused by the strong self-focusing effect with the formation of a filament. The strong increase of the pump intensity leads to the violation of the optimum QPM condition, which terminates the frequency conversion. Figure 4 (b) and (d) illustrates the well known dynamics of the formation of a filament after approximately ~ 50 cm propagation. As seen the combined action of the optical Kerr effect, multiphoton absorption and ionization leads to focusing and defocusing cycles with very small quasi-periodicity [36]. This highly dynamic process leads to aperiodic spikes in the free electron density (Fig. 4. (c)) and recurrent, aperiodic intensity variations (Fig. 4 (b)) of the fundamental (blue curve) and the TH (red curve). The resolution in the numerical simulation of Fig. 4. is about 0.2 mm.

Next, we investigate TGH with a higher pump energy of 0.1 J with the duration of $\tau_\omega = 1$ ps, radius $r_\omega = 0.1$ cm ($I_o \approx 6$ TW/cm^2) and the sound wave amplitude $p = 0.01$ atm. As can be seen from the Fig. 5. the conversion efficiency of THG up to $\approx 0.02\%$ can be obtained. However, in this case a multifilamentation takes place. It appears because the input peak power ($P_\omega \approx 93$ GW) is much larger than the critical power ($P_{crit} \approx 0.9$ GW) [36].
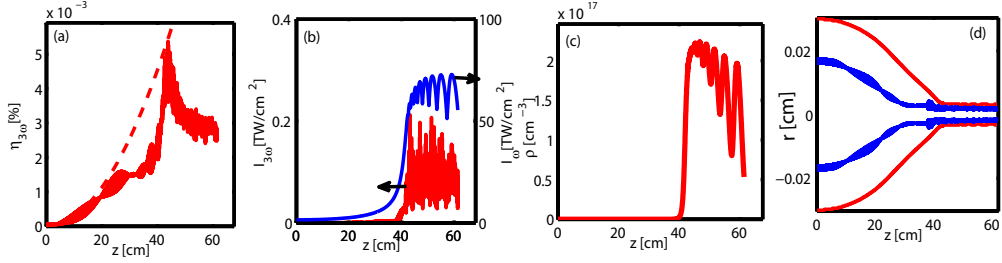
Figure 4: THG for a 1.4 ps pump pulse at 400 nm with 3 mJ energy. In (a) the conversion efficiency calculated analytically by Eq. (8) (dashed) and numerically (solid); in (b) the evolution of the peak intensity of the fundamental (blue) and the TH (red); in (c) the maximum electron density and in (d) the change of radii of the fundamental (red) and the TH (blue) are presented.
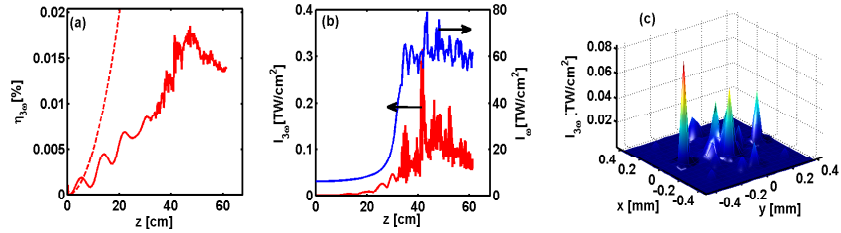

Figure 5: THG for a 1 ps pump pulse at 400 nm with 0.1 J energy. In (a) the conversion efficiency calculated analytically by Eq. (8) (dashed) and numerically (solid); in (b) the evolution of the peak intensity of the fundamental (blue) and the TH (red); in (c) the spatial intensity profile of the TH at the output are presented.

3.3 Sub-20 fs VUV pulse generation by using chirped 400 nm pump pulses

The method under consideration can be combined with a stretching of the pump pulses to much longer durations. This allows to reduce the peak intensity to a range where deleterious nonlinear effects do not play a role. Using negatively chirped pump pulses the generated chirp of the TH can be compensated by normal dispersive elements. In the simulation shown in Fig. 6 and Fig. 7 we assume a negatively chirped pump pulse with a duration of $\tau_\omega = 1$ ps and 0.3 mJ energy obtained after phase-modulation from a bandwidth-limited one of 20 fs duration. The beam radius is $r_\omega = 0.25$ cm, the input intensity is $I_o \approx 2.87$ TW/cm^2 and the sound amplitude is $p = 0.01$ atm. As one can see, the conversion efficiency is limited to the same level as in the previous example. However, the duration of both pump and TH pulses decrease significantly because of chirp compensation due to propagation in the normal-dispersive argon gas (Fig. 7(a)). The duration of the generated VUV pulse at 133 nm is reduced down to 18 fs (Fig. 7(c)) and its pulse energy is ~ 3 μJ. This self-compression is caused by a chirp compensation during propagation due to normal dispersion of the gas.
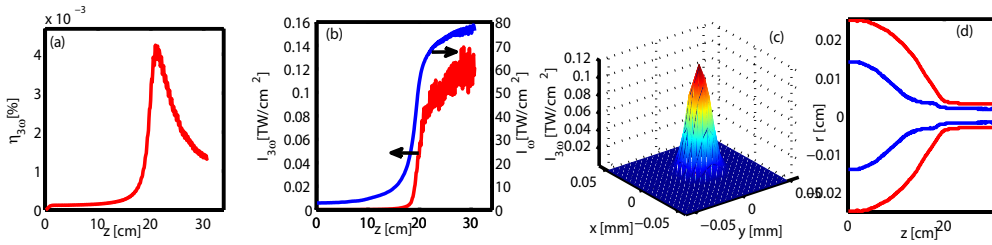

Figure 6: THG for a negatively chirped pump with the energy of 3 mJ. (a) The THG efficiency $\eta_{3\omega}$ in dependence on z; (b) Peak intensity of the fundamental (blue) and the TH (red) pulses versus z; (c) Spatial profile of the TH at the output; (d) Change of radii of the fundamental (red) and TH (blue) with z.
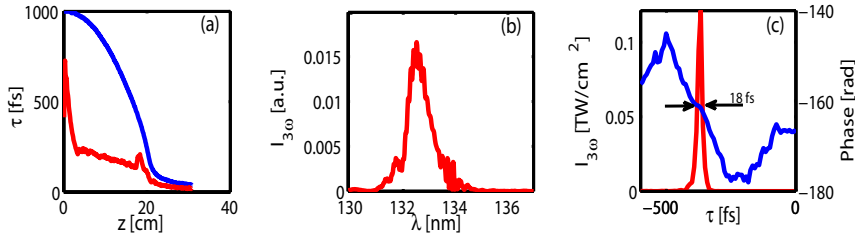

Figure 7: Evolution of the pulse duration (a) as well as the spectral (b) and temporal (c) shapes of the TH pulse at the output for the parameters of Fig.6. Blue and red curves in (a) refer to the fundamental and the TH pulses, respectively. In (c) blue curve represents the phase of the TH.

Finally, we study chirped THG in the high energy regime with chirped pump pulses at 400 nm and the energy of 0.1 J, radius of $r_\omega = 0.1$ cm and the input peak intensity $I_o \approx 6$ TW/cm^2. The pump pulse duration is 1 ps stretched by a phase-modulation from 50 fs ($I_o \approx 119$ TW/cm^2). The ultrasound amplitude is $p = 0.01$ atm. Figure 8 shows the results of the numerical simulations for this case. Up to the length of 40 cm the efficiency increases due to QPM by ultrasound and the rapid increase of the pump intensity because of self-focusing (Fig.

8(a) and (b)). Here we also see that the TH beam is split into two main filaments and a weak background (Fig. 8(c)). The temporal shape of the TH pulse at the output remains relatively well-defined, with a pulse duration as small as 16 fs (see Fig. 8(d)).
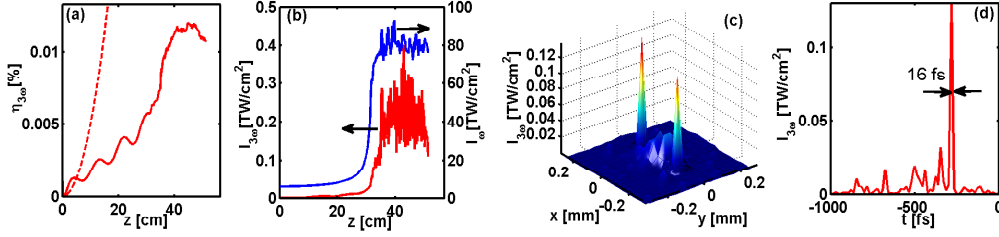

Figure 8: THG for a negatively chirped pump with energy of 100 mJ using . (a) THG efficiency in dependence on z; (b) Peak intensity of the fundamental (blue) and the TH (red); (c) Spatial profile of the TH at the output; (d) Temporal shape of the TH at the output.

4   Conclusions

In conclusion, in this paper we numerically studied quasi-phase matching of THG in a cell filled with a noble gas in which, by a piezoelectric transducer, an ultrasound wave is generated, changing periodically the gas pressure and therefore the third-order nonlinear coefficient in the axial direction. In this scheme quasi-phase matching is realized by choosing an appropriate ultrasound frequency in the range from 22 kHz to 300 kHz compensating the phase-mismatch between the pump pulse and its TH. Using a comprehensive numerical model taking into account third-order nonlinearity, multi-photon ionization, plasma effects, dispersion, diffraction and the modulation of the pressure by the ultrasound, we studied UV pulse generation at 266 nm with 800 nm pump and VUV pulse generation at 133 nm by 400 nm pump pulses with moderate (3 mJ) as well as with high pulse energy (0.1-1 J). This method can also be used for the generation of ultrashort VUV pulses by ultrashort chirped pump pulses stretched to a longer pulse duration to avoid walk-off and destructive nonlinear effects. By using negatively chirped pump pulses the chirp of both the pump pulse and the TH can be compensated during propagation by the normal dispersion of the gas. We predict that in such way almost bandwidth-limited VUV pulses at 133 nm with a duration below 20 fs can be generated without the need of external chirp compensation at the output.

Despite of the conceptual simplicity of the proposed method for frequency conversion in gases, we found important physical limitations restricting the efficiency of THG. The main problem is that if the intensity of the pump pulse is changed during propagation due to self-focusing or other effects, the effective ultrasound frequency for QPM is also modified. This leads to a cessation of further increase of the TH. In a similar way for higher pump intensities ionization of the gas results in a plasma contribution to the refractive index also influencing the optimum ultrasound frequency. As a result the effective interaction length is restricted by these effects, resulting in rather small conversion efficiency, depending on the working conditions. In principle these effects can be compensated at least partially by using a gas cell with varying background

9

pressure in the axial direction or using ultra-sound waves containing several frequencies. The study of such modified scheme is beyond the scope of the present work. Finally, it should be noted that this method of QPM in isotropic gases by using of ultrasound can also be applied for other nonlinear processes such as four-wave mixing or high-order harmonic generation. These issues will be studied in forthcoming work.

Acknowledgments

References

[1] J. W. Ward and G. H. C. New, "Ultrabroadband phase-matched optical parametric generation in the ultraviolet by use of guided waves," Phys. Rev. **185,** 57–72 (1969).

[2] G. Bjorklund, "Effects of focusing on third-order nonlinear processes in isotropic media," IEEE J. Quantum Electron. **QE-11,** 287–296 (1975).

[3] R. Eramo and M. Matera, "Third-harmonic generation in positively dispersive gases with a novel cell," Appl. Opt. **33,** 1691–1696 (1994).

[4] T. Tamaki, K. Midirika, and M. Obara, "Phase-matched third-harmonic generation by nonlinear phase shift in a hollow fiber," Appl. Phys. B **67,** 59–63 (1998).

[5] D. S. Bethune and C. T. Retter, "Optical harmonic generation in nonuniform gaseous media with application to frequency tripling in free-jet expansions," IEEE J. Quantum Electron. **QE-23,** 1348–1360 (1987).

[6] C. W. Siders, N. C. Turner, M. C. Downer, A. Babine, A. Stepanov, and A. M. Sergeev, "Blue-shifted third-harmonic generation and correlated self-guiding during ultrafast barrier suppression ionization of subatmospheric density noble gases," J. Opt. Soc. Am. B **13,** 330–336 (1996).

[7] S. Backus, J. Peatross, Z. Zeek, A. Rundquist, G. Taft, M. M. Murnane, and H. C. Kapteyn, "16-fs, 1-μJ ultraviolet pulses generated by third-harmonic conversion in air," Opt. Lett. **21,** 665–667 (1996).

[8] S. A. Trushin, K. Kosma, W. Fub, and W. E. Schmid, "Sub-10-fs supercontinuum radiation generated by filamentation of few-cycle 800 nm pulses in argon," Opt. Lett. **32,** 2432–2434 (2007).

[9] N. Akozbek, A. Iwasaki, A. Becker, M. Scalora, S. L. Chin, and C. M. Bowden, "Third-Harmonic Generation and Self-Channeling in Air Using High-Power Femtosecond Laser Pulses," Phys. Rev. Lett. **89,** 143901 (2002).

[10] N. Kortsalioudakis, M. Tatarakis, N. Vakakis, S. D. Moustaizis, M. Franco, B. Prade, A. Mysyrowicz, A. A. Papadogiannis, A. Couairon, and S. Tzortzakis, "Enhanced harmonic conversion efficiency in the self-guided propagation of femtosecond ultraviolet laser pulses in argon," Appl. Phys. B **80,** 211–214 (2005).

[11] X. Yang, J. Wu, Y. Peng, Y. Tong, S. Yuan, L. Ding, Z. Xu, and H. Zeng, "Noncollinear interaction of femtosecond filaments with enhanced third harmonic generation in air," Appl. Phys. Lett. **95,** 111103 (2009).

[12] S. Suntsov, D. Abdollahpour, D. G. Papazoglou, S. Tzortzakis, "Efficient third-harmonic generation through tailored IR femtosecond laser pulse filamentation in air," Opt. Express **17**, 3190–3195 (2009). `http://www.opticsinfobase.org/oe/abstract.cfm?uri=oe-17-5-3190`

[13] S. Suntsov, D. Abdollahpour, D. G. Papazoglou, S. Tzortzakis, "Filamentation-induced third-harmonic generation in air via plasma-enhanced third-order susceptibility," Phys. Rev. A **81**, 033817 (2010).

[14] Y. Liu, M. Durand, A. Houard, B. Forestier, A. Couairon, A. Mysyrowicz, "Efficient generation of third harmonic radiation in air filaments: A revisit," Opt. Commun. **284,** 4706–4713 (2011).

[15] C. G. Durfee, S. B. Margaret, M. Murnane, and H. C. Kapteyn, "Ultrabroadband phase-matched optical parametric generation in the ultraviolet by use of guided waves," Opt. Lett. **22,** 1565–1567 (1997).

[16] P. Tzankov, O. Steinkellner, J. Zheng, M. Mero, W. Freyer, A. Husakou, I. Babushkin, J. Herrmann, and F. Noack, "High-power fifth-harmonic generation of femtosecond pulses in the vacuum ultraviolet using a Ti:sapphire laser," Opt. Express **15**, 6389–6395 (2007). `http://www.opticsinfobase.org/abstract.cfm?URI=oe-15-10-6389`

[17] I. V. Babushkin and J. Herrmann, "High energy sub-10 fs pulse generation in vacuum ultraviolet using chirped four wave mixing in hollow waveguides," Opt. Express **16**, 17774–17779 (2008).

`http://www.opticsinfobase.org/oe/abstract.cfm?uri=oe-16-22-17774`

[18] J. A. Armstrong, N. Bloembergen, J. Ducuing, and P. S. Persham, Ïnteractions Between Light Waves in a Nonlinear Dielectric,"Phys. Rev. **127,** 1918–1939 (1962).

[19] M. M. Fejer, G. A. Magel, D. H. Jundt, and R. L. Byer, "Quasi-Phase-Matched Second Harmonic Generation: Tuning and Tolerances," IEEE J. Quantum Electron. **QE-28,** 2631–2654 (1992).

[20] A. Paul, R. A. Bartels, R. Tobey, H. Green, S. Weiman, I. P. Christov, M. M. Murnane, H. C. Kapteyn, and S. Backus, "Quasi-phase-matched generation of coherent extreme-ultraviolet light," Nature (London) **421,** 51–54 (2003).

[21] S. L. Voronov, I. Kohl, J. B. Madsen, J. Simmons, N. Terry, J. Titensor, Q. Wang, and J. Peatross, "Control of Laser High-Harmonic Generation with Counterpropagating Light," Phys. Rev. Lett. **87,** 1339021 (2001).

[22] X. Zhang, A. L. Lytle, T. Popmintchev, X. Zhou, H. C. Kapteyn, M. M. Murnane, and O. Cohen "Quasi-phase-matching and quantum-path control of high-harmonic generation using counterpropagating light," Nature Phys. **3,** 270–275 (2007).

[23] J. Herrmann, Äpparatus and method for amplification and frequency transformation of laser radiation using quasi-phase matching of four-wave mixing,"Patent: DE102009028819A1 (2011).

[24] T. G. Leighton, "What is ultrasound?" Prog. in Bioph. and Molec. Biol. **93**, 3–83 (2007).

[25] A. Holm and H. W. Persson, "Optical diffraction tomography applied to airborne ultrasound," Ultrasonics **31**, 259–265 (1993).

[26] J. A. Gallego-Juarez and L. Gaete-Garreton, "Experimental study of nonlineairity in free progressive acoustic waves in air at 20 kHz," J. De Phys. **40,** C8-336–340 (1979).

[27] H. Tijdeman, "On the propagation of sound wave in cylindrical tubes," J. of Sound and Vibr. **39**, 1–13 (1975).

[28] E. Rodarte, G. Singh, N. R. Miller, and P. Hrnjak, "Sound attenuation in tubes due to visco-thermal effects," J. of Sound and Vibr. **231**, 1221–1241 (2000).

[29] T. D. Rossing, *Handbook of Acoustics* (Springer, 2007).

[30] M. Iskhakovich, *General Acustics* (Nauka, Moscow, 1973).

[31] L. J. Bond, C. Chiang, and C. M. Fortunko, "Absorption of ultrasonic waves in air at high frequencies (10-20 MHz)," J. Acoust. Soc. Am. **92,** 2006–2015 (1992).

[32] Z. Song, Y. Qin, G. Zhang, S. Cao, D. Pang, L. Chai, Q. Wanga, Z. Wangb, and Z. Zhang, "Femtosecond pulse propagation in temperature controlled gas-filled hollow fiber," Opt. Commun. **281,** 4109–4113 (2008).

[33] M. Mlenjnek, E. M. Wright, and J. V. Moloney, "Femtosecond pulse propagation in argon: A pressure dependence study," Phys. Rev. Lett. **58,** 4903–4910 (1998).

[34] A. Couairon, M. Franco, G. Meťchain, T. Olivier, B. Prade, and A. Mysyrowicz, "Femtosecond filamentation in air at low pressures: Part I: Theory and numerical simulations," Opt. Commun. **58,** 265–273 (2006).

[35] G. P. Agrawal, *Nonlinear fiber optics* (Academic press, USA, 2001).

[36] A. Couairon and A. Mysyrowiczb, "Femtosecond filamentation in transparent media," Phys. Repor. **441,** 47-189 (2007).